Design and FE Analysis of an Outer-Rotor PM Generator for Directly-Coupled Wind Turbine Applications

Jian Yi Chen
Student Member

Chem Nayar
IEEE, Senior Member

Longya Xu
IEEE Senior Member, IEEE

Centre for Renewable Energy Systems Technology
Curtin University of Technology
Perth, 6845
Australia

Dept. of Electrical Engineering
The Ohio State University
Columbus, OH 43210-1272
U. S. A

Abstract - This paper presents the design and Finite Element (FE) analysis of a permanent magnet (PM) generator using Neodymium-Iron-Boron magnets for directly-coupled wind turbine applications. To accomplish the goal of small size and light weight with an extra-low speed for direct coupling, the outer rotor structure is applied. The simple magnetic equivalent circuit approach is used for initial design iteration, and the finite element method applied to analyze the detailed characteristics. Comprehensive experimental tests were conducted to verify the theoretical predictions. A good agreement between the theoretical work and testing results was achieved.

1. INTRODUCTION

Recent study shows a great demand for small to medium rating (up to 20 kW) wind generators for stand-alone generation-battery systems in remote areas. The type of generator for this application is required to be compact and light so that the generators can be conveniently installed at the top of the towers and directly coupled to the wind turbines. Compared to a conventional, gearbox coupled wind turbine generator, directly coupled generators has a series of advantages, such as a much reduced size of the overall system, a rather low installation and maintenance cost, flexible control method, quick response to the wind fluctuation and load variations, etc. However, a directly coupled generator needs to have a very low-speed operation to match the wind turbine speed and, at the same time, to produce electricity in a normal frequency range (30-80 Hz). According to the electric machine design principles, this implies a very bulky generator with a very big pole number.

Potentially, permanent magnet (PM) generators offer a high efficiency in operation, and a simple and robust structure in construction because no field current and winding are used. The attractiveness of PM generators is further enhanced by the availability of high-energy permanent magnet materials such as Neodymium-Iron-Boron. This paper presents a novel PM generator design to fully explore the potentials of high-energy PM machines in directly coupled wind energy applications [1-4]. In particular, an innovative outer-rotor structure is adopted to cope with various difficulties in designing a directly coupled wind turbine generator. In a normally designed inner rotor PM generator for gearbox coupled applications, the pole number is low and the magnets can be arranged on the rotor. In order to produce normal frequencies at very low speeds for direct coupling to the wind turbine, the PM generator needs a very large pole number, resulting in a design of substantially enlarged diameter and high cost. To be economically competitive, the design of low-speed, large-diameter generators has to be optimized in terms of cost, power density, and efficiency. As will be discussed in this paper, the structure of outer-rotor displays uniqueness to meet such requirements.

Important design principles associated with the outer rotor structure are discussed along with the critical design constraints. The simple magnetic equivalent circuit approach is used for a quick and iterative design and optimization. The finite element method is applied to analyze the details of the outer rotor PM generator. Comprehensive experimental tests were conducted to verify the characteristics of the prototype generator. A comparison between the theoretical work and testing results is presented to demonstrate the effectiveness of design principles and methodologies.

2. FEATURES OF OUTER-ROTOR STRUCTURE

The most salient feature of the designed PM generator is the outer-rotor structure as shown in Fig.1.

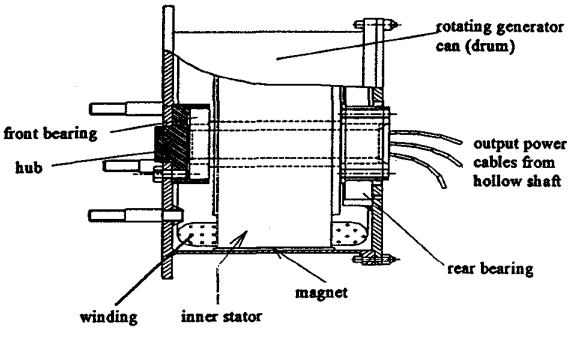

Fig. 1 Axial cutaway view of the generator

As can be noticed, the wound stator is stationary, located in the center of the machine while the magnets are mounted evenly along the inner circumference of the rotating drum supported by the front and rear bearings. In fact, this rotating steel rotor drum plays significant multi-functions: it i)

0-7803-4943-1/98/$10.00 © 1998 IEEE

supports magnetic poles, ii) forms part of magnetic path for the main flux, iii) provides the direct joint between wind turbine and the generator, and iv) forms the protective cover to prevent the generator from environmental hazards. Several advantages can be identified easily from the illustrated outer-rotor structure:

a) The blades of the wind turbine can be conveniently bolted to the front face of the drum to realize the direct coupling between the wind turbine and the PM generator;

b) Because of the enlarged periphery of the out-rotor drum, the multi-pole structure can be easily accommodated;

c) Due to the multi-pole structure, the total length of the magnetic path is reduced. This makes not only an effective utilization of the permanent magnets but also a noticeable height reduction of the rotor yoke, resulting in a significantly reduced total volume and weight.

d) The coil pitch equals to the slot pitch so that the end winding is shorter and correspondingly, copper loss is lower than those in a long pole pitch machine.

Furthermore, with the ratio of the rotor diameter to the magnet width large enough, a minor air gap between the inner arc of the drum and the flat magnet surface will not be significant, resulting in a much simplified process of machining and mounting of the permanent magnets. Therefore, a small pole pitch and larger pole number is favorably accommodated by the outer-rotor structure and a cost-effective, directly coupled PM generator can be made. In the actual design, all of the radially magnetized magnets are squarely shaped and evenly placed to the inner periphery of the rotor drum. While the generator is running, the centrifugal force of the magnets applies a pressure to the bonding media. Thus, the reliability of the glued joints become higher. As exposed to the natural wind flow, the outer-rotor has a much reduced temperature rise than the stator. Additionally, the simple outer-rotor structure makes the PM generator compact, light and rugged, and easy to be installed at the top of a high tower.

3. SPEED AND DESIGN CONSTRAINTS

The critical factors, affecting the main dimensions of the PM generator, and the special design constraints due to the outer rotor structure are discussed in this section.

A. Determining Nominal Speed

The nominal speed of the PM generator, which largely determines the overall size of the generator, can be determined from the wind energy assessment equation. With the radius R of blades, a wind turbine can develop power:

$$P_t = \frac{1}{2} C_p \rho \pi R^2 v^3 \quad (1)$$

where C_p is the conversion efficiency with a typical value of 0.45 or below, ρ the air density and v the wind velocity. A power coefficient can be defined as the ratio of the turbine's blade tip speed to the wind speed given below

$$\beta = v_t / v = \omega R / v \quad (2)$$

where v_t is the turbine blade tip speed and ω the turbine shaft angular speed. Detailed analysis shows that a single maximum C_{pmax} occurs when β takes a particular value β_{max}[8]. Obviously, if the turbine is to extract maximum power from the wind, the shaft speed should vary accordingly to the wind speed. When the turbine is running at β_{max}, the output power from the turbine is,

$$P_t = (\frac{1}{2} \rho \pi C_{pmax} R^2) v^3 \quad (3)$$

The terms in the bracket are considered constant for a given wind turbine, and hence the output power varies as the cube of the wind speed. P_t can be alternatively expressed in terms of ω as

$$P_t = (\frac{1}{2} \rho \pi C_{pmax} R^5 / \beta_{max}^3) \omega^3 \quad (4)$$

If a mean annual wind speed of 7.1 m/s is derived from the previous statistic distribution of wind speed in the areas of Western Australia, a speed of 170 rpm can be selected as the nominal speed for the wind turbine as well as the PM generator. For the nominal frequency of 68 Hz, the permanent magnet has to have 48 poles.

B. Other Critical Design Constraints

- *Temperature Rise*

Since it is exposed to the open-air in remote locations, the PM generator is required completely enclosed for protection against possible damages caused by storm, sun radiation, dust, insects, chemical pollution, etc.. Therefore, there is almost no direct ventilation between inside and outside of the rotor drum and the only heat dissipation is through the drum outer surface. Due to the multi-pole structure the iron loss is larger than a normally designed electric machine. So, the heat generated by armature and other losses may cause a noticeable temperature rise. A maximum ambient temperature of 50°C is assumed and the glue material binding the magnets is able to withstand 120°C. Thus, a constraint of maximum temperature rise of 70°C is imposed for the full load condition. All of the thermal sources must be catered for the assumed condition.

- *Demagnetization*

The magnets can be partially demagnetized by over current and/or excessive temperature. The PM generator has to be

specified to suffer no more than a tolerable demagnetization even at a possible maximum current and temperature. In addition, the magnetic design should ensure that the magnets are safe with demagnetization currents applied at all possible orientations.

4. ELECTROMAGNETIC DESIGN

An iterative magnetic circuit method is employed to search for a proper operating point of the magnet in no- and full load conditions. The method involves discretization of the magnetic flux loop path that is shown by the cross-section of the generator in Fig. 2. The objective of iteration is to produce an optimized magnetic structure with a low cost. The calculation is based on a smooth, non-slotted outer stator surface since the slot effect is accounted for by the traditional Carter coefficient approach.

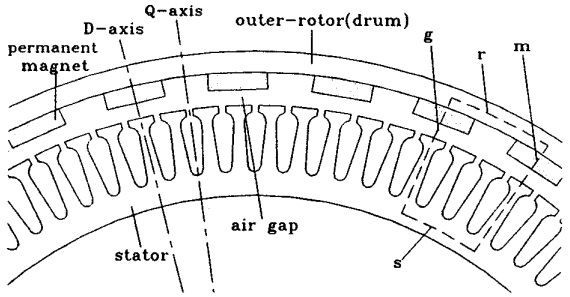

Fig. 2 Cross section of PM generator

A. *No-Load Operating Point*

When the PM generator is working in no-load condition, the air gap flux is solely contributed by the magnets. It is assumed that the demagnetization curve of the permanent magnets is stable with a single valued relationship between B and H. Namely, the demagnetization is reversible within the range of operation. Although the Nd-Fe-B permanent magnet has its demagnetization curve in the second quadrant in B-H plane, H is treated as a positive value for convenience of calculation. For a magnet with given geometry, it is more convenient to use Φ-F curve which can be directly derived from its B-H curve using

$$\Phi = BA_m \text{ and } F = Hh_m$$

where A_m and h_m are the face area and height of the magnet. The obtained Φ-F characteristic is shown in Fig. 4. Note that the Φ-F demagnetizing curve is linear with intercepts of $\Phi_r = B_r A_m$ and $F_c = H_c h_m$. Hence,

$$\Phi = -(\Phi_r / F_c)F + \Phi_r \qquad (5)$$

The ratio, Φ_r / F_c, can be interpreted as the permeance of the magnet. If paths are considered for both the main and leakage flux, a balance between the reluctance drops and the magnet MMFs guarantees that

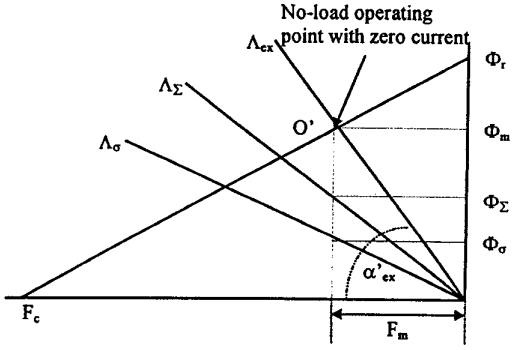

Fig. 3 No-load operating point of magnet

$$\begin{aligned}\Phi_m &= \Phi_\Sigma + \Phi_\sigma \\ &= F_m/(R_g+R_s+R_r) + F_m\Lambda_\sigma \\ &= F_m(\Lambda_\Sigma + \Lambda_\sigma)\end{aligned} \qquad (6)$$

where $R_g+R_s+R_r$ is the total reluctance due to the gap, stator core and rotor core and Λ_Σ and Λ_σ are the permeance for the main flux and leakage flux respectively. The main flux path within a pair of poles consists of rotor yoke, two magnets, two sections of air gap, stator teeth and yoke. The total permeance Λ_{ex} of the entire magnetic circuit can be expressed as

$$\Lambda_{ex} = \Phi/F_m = \Lambda_\Sigma + \Lambda_\sigma \qquad (7)$$

Λ_{ex}, the total permeance of no-load magnetic circuit, represents the external effect to the magnet. The operating point corresponding to the no-load condition is plotted as the intersection O' of the no-load line with the demagnetizing curve shown in Fig. 3. The coordinate Φ_m on Φ-axis represents the total flux coming out from a magnet face. The angle of the no-load line is

$$\alpha'_{ex} = \arctan \Lambda_{ex} \qquad (8)$$

The two lines with the slopes of main permeance Λ_Σ and leakage permeance Λ_σ are also shown in the figure. The proper operating point can be adjusted by applying the iterative method to change the dimensions of the permanent magnets, which essentially changes the position of the PM demagnetization curve, and the geometry of the stator and rotor lamination, which essentially determines the slope of no-load line Λ_{ex}.

Although it is convenient to determine the no-load (open-circuit) operating point by using magnetic Φ-F characteristic and permeance lines, it is very direct to use the B-H curve to compute the magnetic structure without considering the

effect of different geometry of magnets. In the B-H domain, a relative parameter p_{ex} can be defined to replace Λ_{ex},

$$p_{ex} = \Lambda_{ex} (h_m/A_m) \tag{9}$$

which is called the normalized permeability line in no-load operation. The concept of normalized permeability will be used later to compute the operation point in full load conditions.

B. *Leakage Flux Permeance*

Leakage flux in the magnetic circuit is caused by the combined MMFs of the magnets and the stator armature current. It is apparent that the calculation of no-load operating point involves the detailed calculation of the leakage permeance in different integral sections. However, a feature of leakage magnetic flux is that the leakage flux lines usually have a relatively long path in air, a linear magnetic media that gives a lot of convenience to find analytic expressions for leakage flux permeance. The leakage permeance related to those sections with various shapes and dimensions, including the paths between stator teeth, rotor poles, and between steel core and magnet, has to be considered. Since the inner-stator has a structure similar to that of a rotor in a normal machine design, we will skip calculating stator slot leakage permeance and others alike.

For the leakage flux permeance between the adjacent poles of the outer-rotor, the important dimensions are shown in Fig. 4.

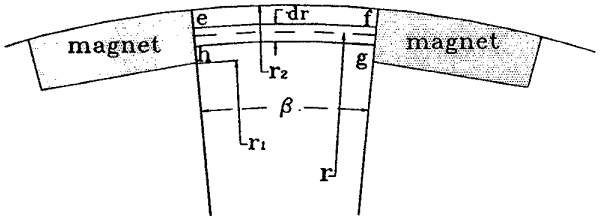

Fig. 4 Leakage flux path between two magnets

The two adjacent sides of the two opposite magnets can be approximately regarded as parts of two extended planes intersecting at the shaft center, with the angle β between them. These two equipotential surfaces have the position radii r_1 and r_2, and axial length l (into the paper). For the element defined by e-f-g-h, the permeance is given by

$$d\Lambda = \frac{\mu_o l dr}{r\beta} \tag{10}$$

Integrating the equation (10) from limits r_1 to r_2, the leakage permeance between the two magnets can be obtained:

$$\Lambda_r = \int_{r_1}^{r_2} d\Lambda = \frac{\mu_o l}{\beta}\int_{r_1}^{r_2}\frac{dr}{r} = \frac{\mu_o l}{\beta}\ln\frac{r_2}{r_1} \tag{11}$$

C. *Full-Load Operating Point*

With the full load current flowing through the armature winding, the magnetic flux of the generator is significantly altered and the operating point varies. The full load magnet operating point has be to positioned in such a way that the magnetic field by the magnets is still adequate and can be completely recoverable for the worst load conditions. The corresponding position of operating point depends on both the direction and amplitude of the armature MMF. The air gap field, set up by the stator armature MMF, possesses direct-axis and quadrature-axis components, which bears a close relationship to the direct- and quadrate-axes inductance, L_d and L_q.

In the case of this PM generator, attention is paid to the demagnetizing component, the negative I_{ds}. It is known that the amplitude of MMF produced by a three-phase d-axis current under one pole is:

$$F_{ad} = \frac{3}{\pi}\frac{2\sqrt{2}W_p k_w}{p} I \tag{12}$$

The field strength due to the armature MMF is:

$$H_{ad} = F_{ad}/h_m = 2.7\frac{W_p k_w}{p h_m} I \tag{13}$$

H_{ad} caused by armature reaction can be directly added to the no-load characteristic. Hence, the no-load line is shifted along the H-axis for a value of H_{ad} and intersects with the magnet demagnetizing curve at point L shown in Fig.5. Note that under the full load, L is the operating point of the magnet. The corresponding coordinate B_{ad} on the B-axis is the flux density.

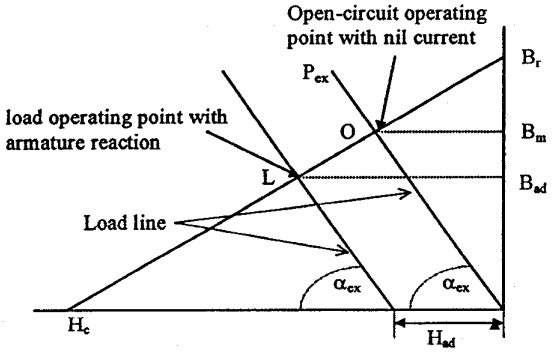

Fig. 5 Load operating point of magnet

To calculate the induced voltage in the load conditions, the radial flux density of the air gap can be decomposed into:

$$B_r(\ell) = \sum_{n=-\infty}^{+\infty}(a_n \cos\frac{n\pi\ell}{\tau} + b_n \sin\frac{n\pi\ell}{\tau}) \tag{14}$$

where a_n,& b_n - coefficients, ℓ - length of the arc of air gap at the centre and τ - pole pitch.

From Eq. (14), the fundamental and other harmonic flux per phase are obtained. So The fundamental and other harmonic EMFs can be found by

$$E_n = 4.44 f W K_{dpn} \Phi_{pn} \qquad (15)$$

where

f - frequency of the power source.
W - number of turns in series per phase.
K_{dpn} - fundamental or harmonic winding factor.

All the design principles and major equations discussed above are summarized and coded into a computer program to design a prototype outer-rotor PM generator and important design results are listed in the table

OD	ID	L	Pole #	Slot #
550 mm	527.3 mm	75 mm	48	144
Turns/ϕ	Circuit	Winding	H_m	A_m
12x24	1	1 Layer	3.5 mm	1875mm^2

5. FINITE ELEMENT ANALYSIS

In the foregoing design and linear analysis, the generator's main dimensions are determined and major performance predicted. However, the permeability of iron core is considered infinite or reluctance neglected, and the main and leakage flux paths or permeance are assumed only being affected the geometry not the MMF levels of the magnets and armature. Also, local magnetic saturation of the lamination is not examined. To validate the design methodologies and predict the performance of the designed PM generator more accurately, Finite Element (FE) analysis is applied to the initial design obtained by the magnetic circuit linear approach. The major concerns in the FE analysis are magnetic flux distribution, winding flux linkages as a function of rotor positions, induced back EMF, and power capability. The 2-D, nonlinear magnetic vector potential equation used is

$$\frac{\partial}{\partial x}(\upsilon \frac{\partial A_z}{\partial x}) + \frac{\partial}{\partial y}(\upsilon \frac{\partial A_z}{\partial y}) = -J_z - J_{zpm} \qquad (16)$$

with J_{zpm} representing the equivalent currents at the magnet boundaries. Only a pole-pitch segment of the entire cross-section is computed because of the lamination symmetry. The computed area is divided into about 5000 discrete elements. The precise nonlinear magnetic characteristic curves of iron core and magnets are used in FE analysis.

A. Flux Distribution

The flux distributions of the PM generator is plotted for both the no- and full load conditions for the rotor rotation of a quarter pole-pitch in each plot in Figs. 6(a) and (b). As can be seen that in no-load condition, the flux distribution is largely symmetric with minor distortion due to the slot effects. Flux density looks reasonable with concentrations on the stator teeth and rotor yoke. Leakage flux between the magnet poles and across stator slots is negligibly small. However, once the PM generator is loaded with a full current, the flux distortion from the symmetric distribution is obvious. Also interesting to be noted is the substantial leakage flux both between the magnet poles and across the stator slots. It is evident that the leakage flux pattern (parameter) is not only determined by the lamination geometry but also by the level of load conditions.

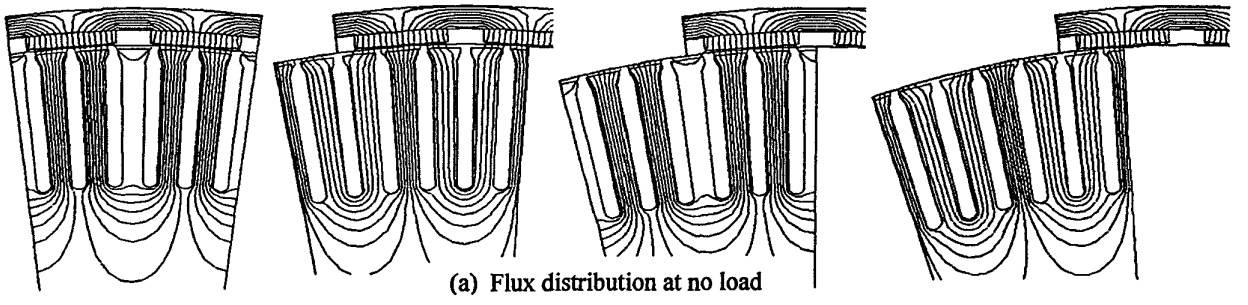

(a) Flux distribution at no load

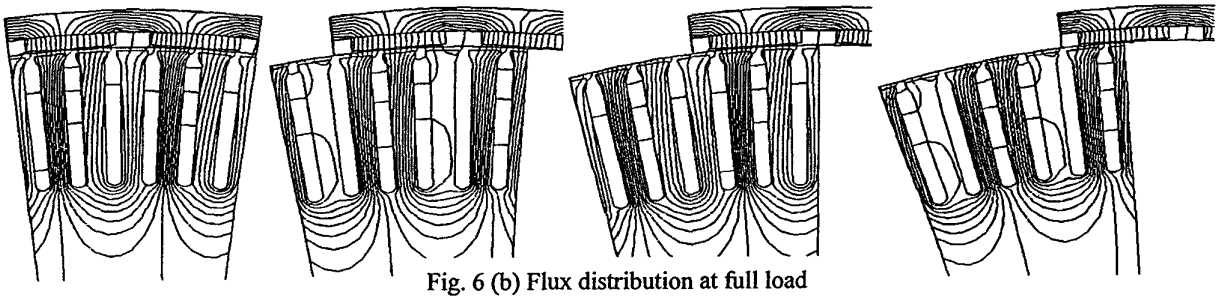

Fig. 6 (b) Flux distribution at full load

B. Winding Flux Linkages and Back EMF

The winding flux linkage λ_{coil} is computed by the equation:

$$\lambda_{coil} = L \int_{a1}^{a2} \frac{\partial A_z}{\partial \ell} d\ell = A_z(a1) - A_z(a2) \qquad (17)$$

where $A_z(a_1)$ and $A_z(a_2)$ are the vector potentials at the locations of the two sides of a coil, a_1 and a_2. Note that the profile of the winding flux linkages determines the waveform of the induced back EMF. Because the slot number per pole per phase of the designed generator is one only with fully pitched single layer windings, it is not difficult to understand that the flux linkage and back EMF of this generator can easily depart from a regular sine wave. The computed winding flux linkages are shown in Figs. 7(a) and (b) and induced back EMF at 170 rpm in Fig. 8.

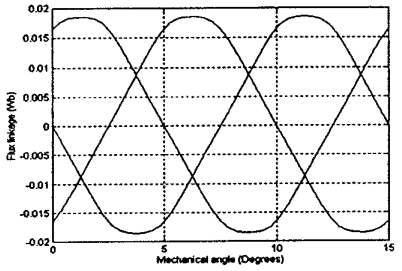

(a) Winding flux linkage at no-load

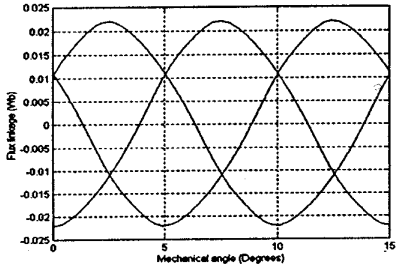

Fig. 7(b) Winding flux linkage at full load

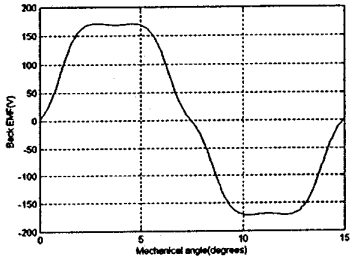

Fig. 8 Induced back EMF at no load

C. Power Capability

Finite element method is also used to investigate the power capability of the designed PM generator. For power computation the load currents are sent into the stator windings and the magnetic field calculated. Then, Maxwell tensor method is applied to obtain torque and power production. Results of the torque and power calculation are given in Fig. 9. Obviously, the design PM generator is fully capable of delivering the expected torque and power.

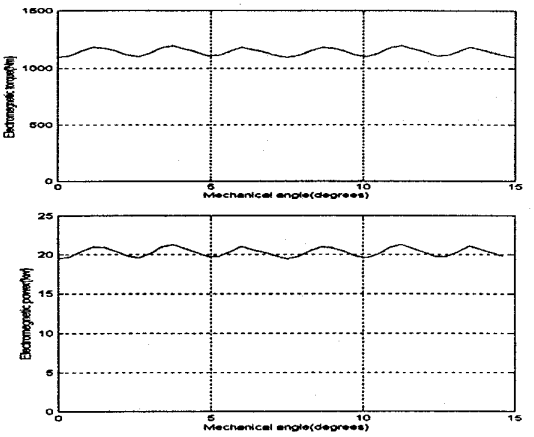

Fig. 9 Torque and power capability at full load

6. EXPERIMENT RESULTS AND COMPARISON

The designed PM generator was built and the photo picture is shown in Fig. 10.

Outer-Rotor

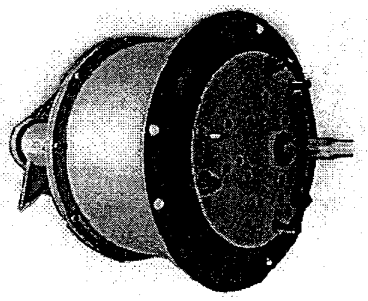

Total Assembly

Fig. 10 Outer Rotor and Assembled PM generator

A comparison between the tested and theoretically predicted performance is made and the results are summarized in this section.

A. Open-Circuit Characteristics

The open-circuit test was conducted under various speeds. The phase voltage waveform (line to neutral) is shown in Fig. 11. As can be noticed, the phase voltage is not quite sinusoidal but rather flat-top. The non-sine waveform is due to the non-sinusoidal winding flux linkage that has been predicted by finite element analysis.

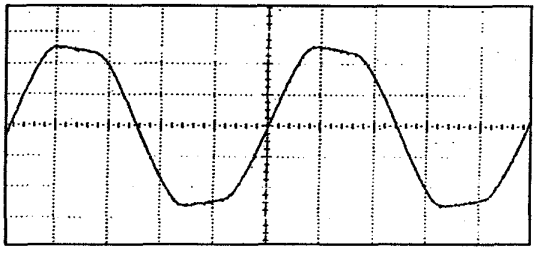

Fig. 11 Waveform of no-load voltage at 170 rpm

The output line-line RMS voltages from computation and measurement are shown in Fig. 12. It is seen that the computed result has a very good agreement with the measured one. The output terminal voltage is linearly proportional to the rotor speed, which also is well predicted by both the magnetic circuit approach and finite element analysis.

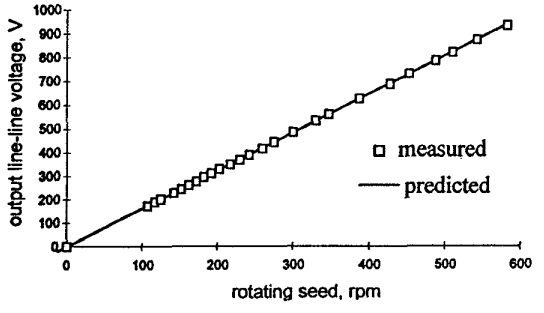

Fig. 12 Open circuit characteristics

A. Performance under Load

The prototype generator is tested with a symmetrical 3-phase resistive load. Varying with the different load resistance in the test, the armature voltage and current waves display significant changes. In the resistive load test, it is found that although the no-load voltage waveform is not a satisfied sinusoid, the voltage waveforms become better sine when the load current increases. The larger the load current is, the more standard sine wave the output voltage tends to be, indicating remarkable reduction of the other harmonics. This trend of waveform improvement occurs when load current increases as a result of either the load resistance reduction at certain frequency, or frequency increasing at certain constant load resistance. Fig. 13 shows the improved voltage waveform with the resistive of 11Ω, at the speed of 170 rpm.

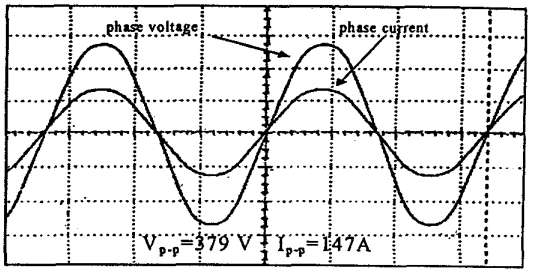

Fig. 13 Output waveform with resistive load

The prediction of voltage variation with the load current at 6 different speeds is shown in Fig. 14.

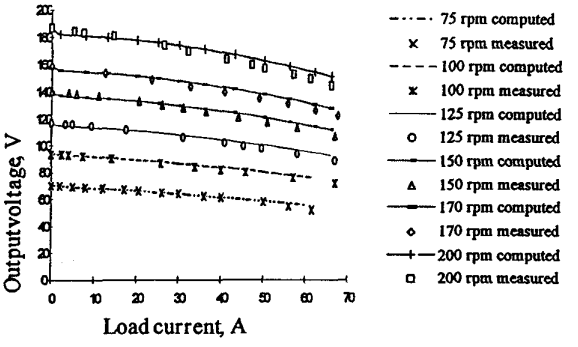

Fig. 14 Predicted and measured voltage regulation

It is well known that at low speeds (frequencies), the inductance has less influence to the voltage regulation than at higher speeds. So, the voltage variation at high speeds is more visible, which is clearly indicated by both the tested and calculated results. The results also indicate that the prediction of voltage variation at lower speed has a better accuracy. This is because i) variation of stator armature resistance due to temperature is not accounted for in the computation, and ii) with frequency increased, load angle and power factor angle vary in a more complicated way.

The power capability of this prototype PM generator is also tested under various loading conditions at 6 different rotational speeds. The output power at each of these speeds is shown in Fig. 15. When the output power of the generator reaches 20 kW at the speed of 170 rpm, the efficiency is about 86% and phase voltage of 134 V. After one hour' full load test, the measured temperature rise of the stator armature was 57°C at the ambient temperature of 31°C. These results

clearly demonstrate the success of the out-rotor PM generator specified in the original design.

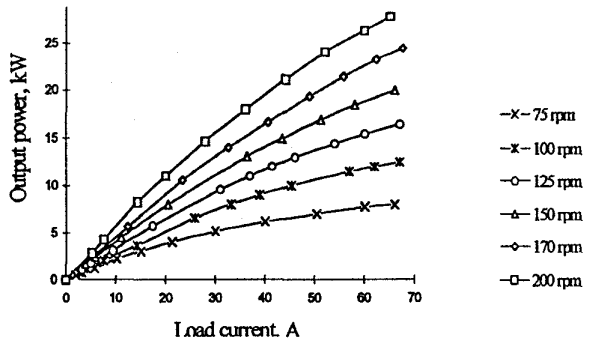

Fig.15 Output power at different speeds

7 CONCLUSIONS

The outer-rotor PM generator described in the paper is used for multi-pole, low speed wind power conversion for a stand-alone application. Design principles and important equations for the outer-rotor, multi-pole permanent magnet generator have been fully developed and utilized for the design and construction of a prototype where high energy Neodymium-Iron-Boron magnet is used. It is verified that a permanent magnet generator made in such a simple construction can operate with good and reliable performance over a wide range of speeds. Using the direct design program for initial iteration and finite element method for detailed analysis and final adjustment, satisfactory results have been achieved. The good agreement between the theoretically predicted and experimentally tested results further prove the correctness of the design principles and the effectiveness of the design methodology.

ACKNOWLEDGMENT

The project was funded by MERIWA. The authors appreciate the cooperation of WestWind, and the assistance for the experiments from Mr P.W. Teo and Mr K.F. Liang. Computation work of finite element analysis done by Mr. B. Wang at The Ohio State University is acknowleged.

REFERENCES

[1] Spooner, E. and Williamson, A.C., "Direct coupled, permanent magnet generators for wind turbine application", IEE Proc.-Electr. Power Appl, 1996, Vol. 143, (1), pp.1-8.

[2] Soderlund, L., Eriksson, J-T., Salonen, J., Vihriala, H. and Perala, R. (1996), "A permanent magnet generator for wind power application", IEEE Transactions for Magnetics, 1996, Vol. 32, No.4, pp.2389-2392.

[3] Nayar, C.V., "Investigation of capacitor-excited induction generators permanent magnet alternators for small scale wind power generation", Renewable energy, 1991, Vol. 1, No.3/4, pp.381-388.

[4] Lampola, P., Perho, J. and Saari, J.: 'Electromagnetic and thermal design of a low-speed permanent-magnet wind generator', Proc. IEEE Powertech conference, Stockholm, 1995, pp.221-215.

[5] L. Xu, L. Ye, L. Zhen and A. El-Antably, "A New Design Concept of Permanent Machine for Flux Weakening Operation", IEEE Transaction on Industry Applications, Vol. 31, No. 2, Mar/April, 1995, pp373-379

[6] L. Xu and L. Ye, "Analysis of a Novel Stator Winding Structure Minimizing harmonic Current and Torque Ripple for Dual Six-Step Converter-Fed High Power AC Machines," IEEE Transactions on Industry Applications, Vol. 31, No. 1, Jan/Feb. 1995, pp. 84-90.

[7] Golding, E.W., (1976), "The Generation of Electricity from Wind Power", E&F Spon Ltd., London.

[8] Johnson, G.L. (1985), "Wind Energy Systems", Prentice-Hall, U.S.A.